

CHAPTER 1

INTRODUCTION

The design strategy of an ideal bone graft, certainly nanocomposite, is not right directions without understanding the fundamentals of bone composition, architecture, and the way in which it is organized. It also is of great importance to know the physical, chemical, and mechanical properties of the bone because they provide quantitative parameters necessary for fabrication of artificial bone replacement implants¹⁻².

When discussing the extraordinary structure of bone is often described in terms of its hierarchical levels of structure. An excellent review was provided by Weiner et al.1998, who broke down the structure of bone into seven levels of hierarchy (Fig. 1.1), starting with nanoscopic platelets of hydroxyapatite (HA) that are oriented and aligned within self-assembled collagen fibrils; the collagen fibrils are layered in parallel arrangement within lamellae; the lamellae are arranged concentrically around blood vessels to form osteons; finally, the osteons are either packed densely into compact bone or comprise a trabecular network of microporous bone, referred to as spongy or cancellous bone¹.

1.1 Bone is a nanocomposite

Bone is an amazing and a true nanocomposite. It is difficult to analyze because it has so many levels of organization. The main constituents of bone are collagen

(20 wt %), calcium phosphate (69 wt %), and water (9 wt %). Additionally, other organic materials, such as proteins, polysaccharides, and lipids are also present in small quantities². Collagen, which can be considered as the matrix, is in the form of small microfibrils. It is difficult to observe distinct collagen fibers because of its net-like mass appearance. The diameter of the collagen microfibrils varies from 100 to 2000 nm. Calcium phosphate in the form of crystallized hydroxyapatite (HA) and/or amorphous calcium phosphate (ACP) provides stiffness to the bone. The HA crystals, present in the form of plates or needles, are about 40–60 nm long, 20 nm wide, and 1.5–5 nm thick³. They are deposited parallel to the collagen fibers, such that the larger dimension of crystals is along the long axis of the fiber (Fig. 1.2). It is worth mentioning that the mineral phase present in the bone is not a discrete aggregation of the HA crystals. It is rather made of a continuous phase which is evidenced by a very good strength of the bone after a complete removal of the organic phase²⁻⁵.

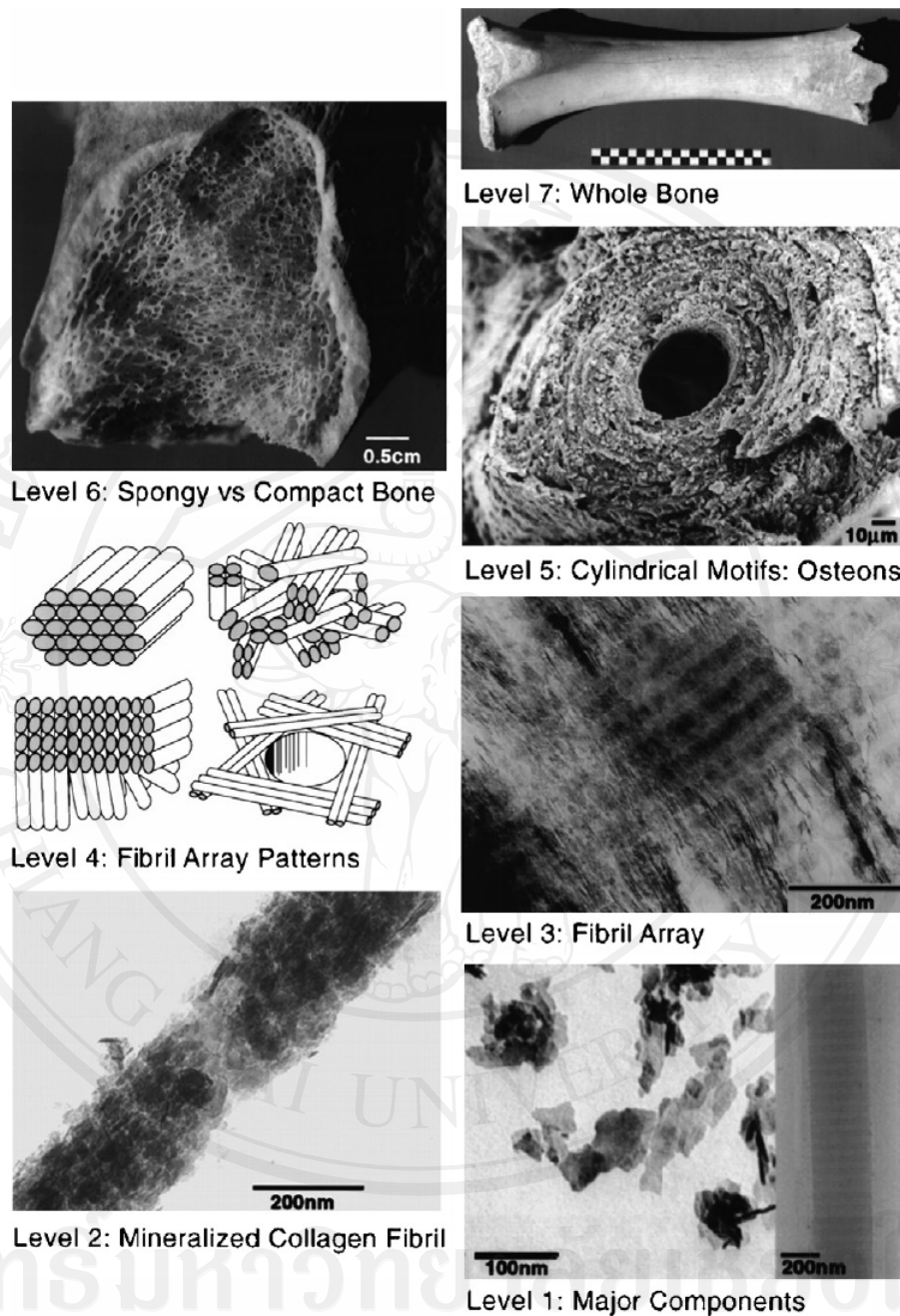


Fig. 1.1 The hierarchical levels of structure found in osteonal bone, as demonstrated by Weiner and Wagner¹.

It was known that mature bone exists in two main forms: compact and cancellous. Hierarchical levels of structural organization in a human compact bone (lamellar) are shown in Fig. 1.2. (Other kinds of compact bone, such as compact

fibrous bone or compact fibrolamellar bone, will not be described here). The mineral-containing fibers are arranged into lamellar sheets (3–7 μm thick) 4–20 lamellae, which are arranged in concentric rings around the Haversian canal, form an osteon. Cross sections of the compact bone, showing cylindrical osteons (also called Haversian system) with blood vessels running along Haversian canals (in the center of each osteon) are shown in Fig. 1.3(a). The metabolic substances can be transported by the intercommunicating systems of canaliculi, lacunae, and Volkman's canals, which are connected with the marrow cavity. The various interconnecting systems are filled with body fluids and their volume can be as high as 19%. Cancellous bone (also called trabecular or spongy bone) is a cellular material consisting of a connected network of rods or plates (Fig. 1.3(b)). Low density, open cell, rod-like structures develop in regions of low stress while high density, closed cell, plate-like structures occur in regions of higher stress⁵.

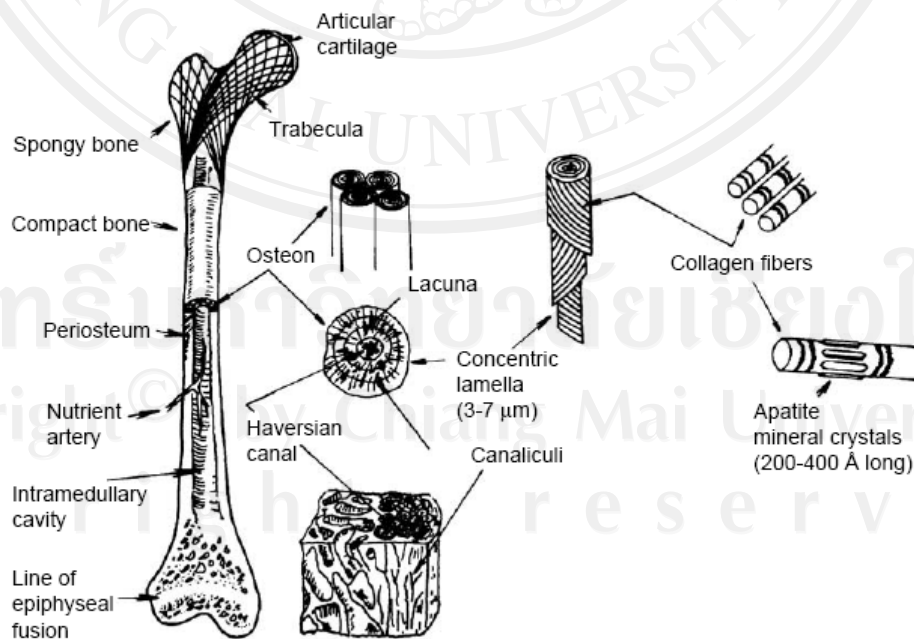


Fig. 1.2 Hierarchical levels of structural organization in a human long bone⁵.

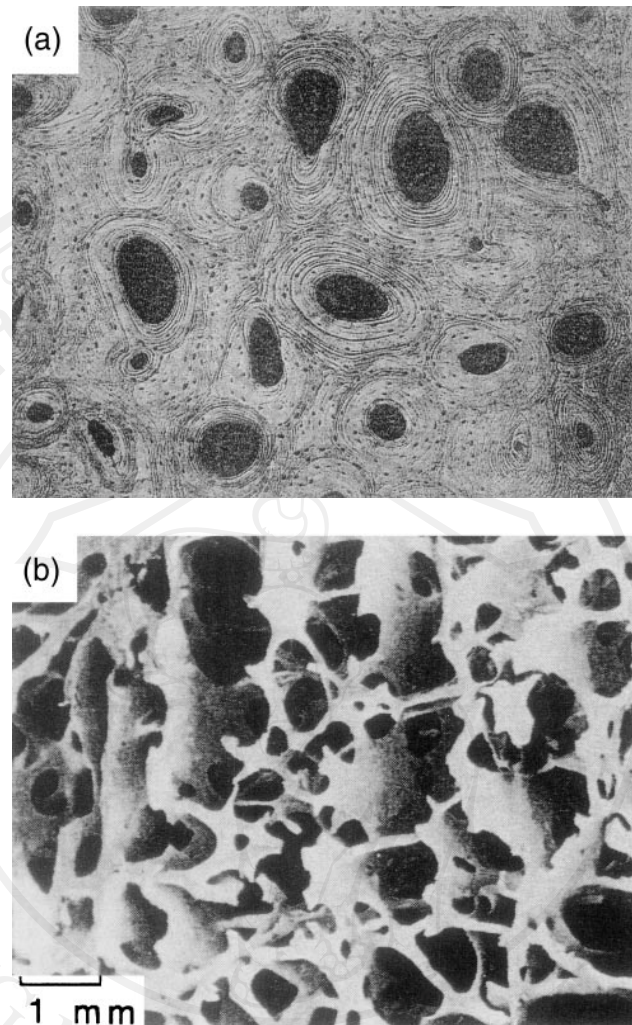


Fig. 1.3 (a) Optical micrograph of transverse cross section showing the microstructure of compact lamellar bone–human femora and (b) Scanning electron micrograph of plate-like cancellous bone with columnar structure⁵.

1.2 Mechanical properties of bone

Organic components of bone (mainly collagen) themselves would behave as a compliant material with high toughness, low modulus, and other properties characteristic for polymers. Inorganic components, i.e., HA crystals, provide appropriate stiffness to the bone. As a ceramic-organic composite, bone exhibits high toughness and relatively high modulus. High toughness is related not only to the

presence of collagen, but also to the complicated fibrous microstructure, described in the previous section. A representative stress-strain curve for bone (Fig. 1.4) shows a linear elastic region, followed by a flat plastic region at about 0.8% strain. Failure occurs at strains up to 3%. It is necessary to mention that bone is a tough material at low strain rates but fractures more like a brittle material at high strain rates. The slope of the stress-strain curve, i.e., the stiffness of the bone, increases with increasing mineral content. Bone exhibits excellent toughness (at low strain rates) mostly due to its hierarchical structure, which stops cracks after little propagation. The main toughening mechanisms seem to be microcracks, which appear in the plastic region of the stress-strain curve, crack deflection, and pullout effects⁵. A typical fracture surface of the bone, showing pullout of individual osteons, is presented in Fig. 1.5.

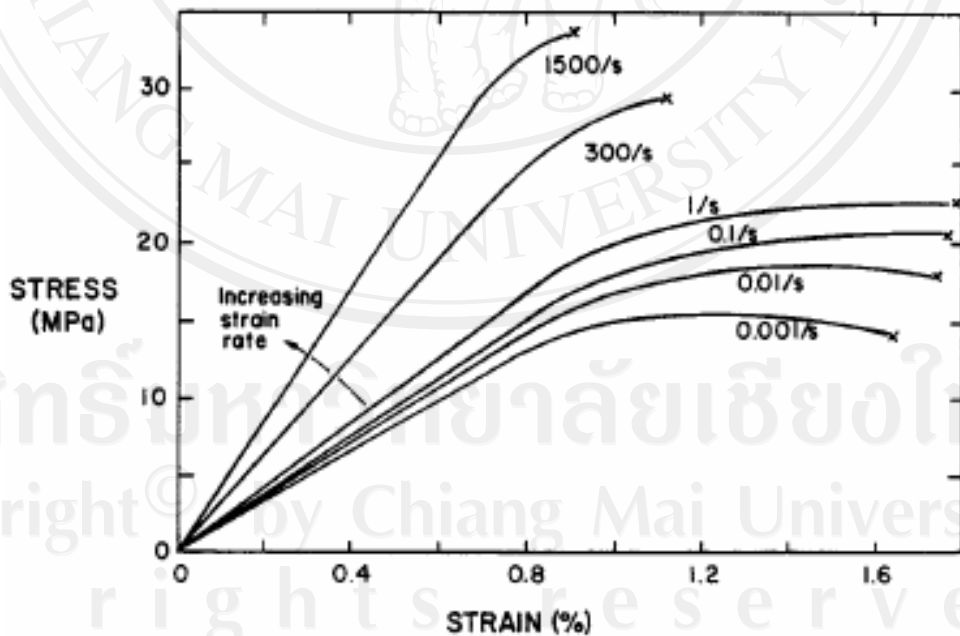


Fig. 1.4 A representative load-deflection curve for human compact bone⁵.

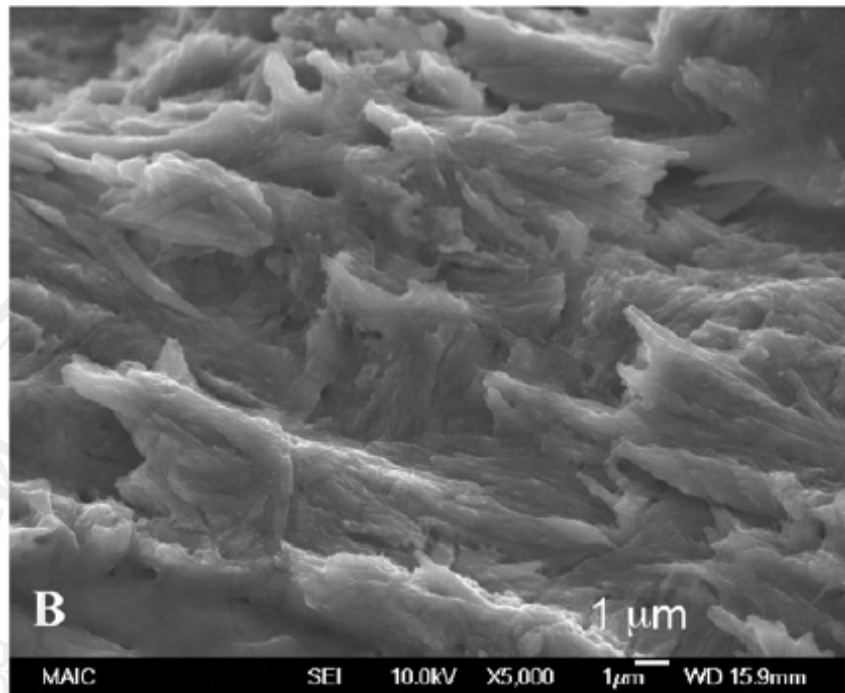


Fig. 1.5 SEM of as-fractured bone¹

The mechanical properties of human compact bone are summarized in Table 1.1. In the case of the cancellous bone, Young's modulus (measured in compression) and compressive strength are in the ranges of 1–2 GPa and 1–100 MPa, respectively. With increasing bone density, both Young's modulus and compressive strength significantly increase. The mechanical properties of bone depend largely on the humidity, mode of applied load, direction of the applied load, and kind of bone. With increasing level of bone mineralization, strength increases and fracture strain decreases. Moreover, strength and other mechanical properties of bone depend upon orientation of the collagen fibers, bone density, and porosity, and the molecular structure and arrangement of its constituent apatite crystals within their collagen matrix. Finally, both strength and volume of the human bone decrease dramatically with age⁵.

Table 1.1 Biomechanical properties of bone⁵

Properties	Measurements	
	Cortical bone	Cancellous bone
Young's modulus (GPa)	14–20	0.05–0.5
Tensile strength (MPa)	50–150	10–20
Compressive strength (MPa)	170–193	7–10
Fracture toughness (MPa m ^{1/2})	2–12	0.1
Strain to failure	1–3	5–7
Density (g/cm ³)	18–22	0.1–1.0
Apparent density (g/cm ³)	1.8–2.0	0.1–1.0
Surface/bone volume (mm ² /mm ³)	2.5	20
Total bone volume (mm ³)	1.4×10^6	0.35×10^6
Total internal surface	3.5×10^6	7.0×10^6

1.3 The present—current status of bone grafting

Bone grafts provide mechanical or structural support, fill defective gaps, and enhance bone tissue formation. They are widely used in orthopedic surgery, plastic surgery, oral and maxillofacial surgery, and dental surgery. It should be noted that bone is the second most transplanted tissue in humans. The graft materials not only replace missing bone but also help the body to regenerate its own lost bone. By this method, bone healing time is reduced and new bone formation strengthens the defective area by bridging grafted materials with host bone. There are a variety of bones grafting methodologies available, which include autografting, allografting, xenografting, and alloplastic or synthetic bone grafting, but each with their own advantages and disadvantages. Autografting is a method in which tissue or organ is transplanted from one site to another site of the same individual. Allografting can be defined as tissue transplantation between individuals of the same species but of non-identical genetic composition. Xenografting is a process of transplanting tissue from

one species to another (e.g., bone from animal to human). As an alternative to the above three types of bone grafts, synthetic substances are gaining much interest for use as bone graft materials. A surgical method that uses synthetic substances to repair or regenerate defective bone tissue is known as alloplastic or synthetic bone grafting. The benefits of synthetic grafts include availability, sterility, cost-effectiveness, and reduced morbidity. The synthetic grafts eliminate some of the shortcomings of autografts or allografts associated with donor shortage and the chance for rejection or transmission of infectious disease. However, the selection of grafting to use is purely dependent on the nature and complication of the bone defects as well as choice of available bone grafts².

1.4 Bone graft materials

Over the past four decades, several biomaterials have been developed and successfully used as bone grafts. Bone and joint substitutes are commonly made of metals, ceramics, polymers, and their composites. In most of the cases, metals and ceramics are used in hard tissue applications, whilst polymers in soft tissue applications due to their mechanical properties. Composites are widely used in both the applications. The mechanical properties of the most commonly used metals, ceramics, and polymers are given in Tables 1.2–1.4, respectively. Metals have been used in clinical orthopedics since the early 1900s. Titanium, stainless steel, Co–Cr, and titanium alloys are notable examples, which are mostly used at load-bearing sites. The elastic modulus of stainless steel and Co–Cr alloys is higher than that of natural bone, i.e., about 10 times greater (see Table 1.2), which gives complications of mechanical incompatibility. Nowadays, titanium and its alloys (e.g., Ti–6Al–4V) are

widely used in load-bearing orthopedic applications. The elastic modulus of these materials is found to be about 5 times greater than natural bone (see Table 1.2). According to Wolff's law, if a stiffer implant material is placed into bone, the bone will be subjected to reduced mechanical stress that gradually leads to bone resorption. This phenomenon is known as stress-shielding. It has been recognized that matching the stiffness of the implant with that of the host tissue limits the stress-shielding effect. Owing to insufficient interfacial bonding between metal implant and host tissue, there is limited osteointegration. In order to improve tissue bonding, HA-coated titanium alloys are widely and successfully used in orthopedic surgery².

Table 1.2 Mechanical properties of metals²

Biometals	Young's modulus (GPa)	Tensile strength (MPa)	Compressive strength (MPa)	Hardness (Vickers, kg/mm)	Fatigue strength (MPa)
Ti	110	300–740	550	120–200	240
Ti-6Al-4V alloy	120	860–1140	860	310	280–600
Stainless steel	190	500–950	600	130–180	260–280
Co-Cr alloy	210	665–1277	655	300–400	200–300

Table 1.3 Mechanical properties of ceramics²

Bioceramics	Young's modulus (GPa)	Tensile strength (GPa)	Compressive strength (GPa)	Fracture toughness (MPa m ^{1/2})	Hardness (HV)	Flexural strength (MPa)	Density (g/cm ³)	Bond strength (GPa)
Alumina	390	0.31	3.9	5.2	2000	390	3.9	300–400
Zirconia ^b	205	0.42	3	12	1150	1300	6	200–500
HA	80–110	0.05	0.4–0.9	0.7–1.2	600	37	3.16	120

Table 1.4 Mechanical properties of polymers²

Polymers	Young's modulus (GPa)	Tensile strength (MPa)
<i>Biodegradable</i>		
Poly(L-lactic acid)	2.7	50
Poly(D,L-lactic acid)	1.9	29
Poly(caprolactone)	0.4	16
Poly(β -hydroxybutyrate)	2.5	36
<i>Non-biodegradable</i>		
Poly(ethylene)	0.88	35
Poly(urethane)	0.02	35
Poly(tetrafluoroethylene)	0.5	27.5
Poly(methyl methacrylate)	2.55	59
Poly(ethylene terephthalate)	2.85	61

Ceramics were introduced to orthopedics during the 1960s. They have high compressive strength and hardness (see Table 1.3); they are also highly biocompatible and tissue responsive. They are also called bioceramics. According to their tissue response, they can be categorized into three types; (i) nearly bioinert (e.g., alumina and zirconia), (ii) bioactive (e.g., HA and bioglass), and (iii) bioresorbable (tricalcium phosphate (TCP)). Alumina was the first clinically used bioceramic material in 1970 owing to its excellent biocompatibility, hardness, strength to resist fatigue, and corrosion resistance. Zirconia has been in use in orthopedics since 1985 in either the pure form or partially yttria-stabilized form. It exhibits fracture toughness greater than alumina. Alumina and zirconia are predominantly used as femoral heads of total hip joints. They do not cause a response from host tissue because they do not chemically or biologically react with surrounding tissues due to their thermodynamic stability. Due to exceptional bioactivity, HA and bioglasses are frequently used as bone graft substitute and as coating-agent on biometallic or biocomposite implants.

Prototypes of such HA based bone graft materials are shown in Fig. 1.5. They elicit a strong interfacial interaction with host tissue due to their bioactivity; thereby they are considered to provide osteointegrative stimuli. However, they are very less bioresorbable. TCP is widely used as a bioresorbable bone graft. The resorbable ceramics provide a framework for new bone tissue to grow while being resorbed, leaving only the new bone behind after complete resorption. However, the rate of bioresorption of TCP is unpredictable and they have certain drawbacks, which include poor mechanical properties (e.g., brittleness and low toughness). Therefore, they are used only in low-weight bearing orthopedic applications. Overall, the ceramics have many advantages that include biocompatibility, easy availability, shapeability, non-toxic, and non-immunogenic².

Polymers are widely used in bone grafting owing to their biocompatibility, design flexibility, functional groups availability, surface modifiability, light weight, and ductile nature. Although they have many desirable characteristics, they exhibit low stiffness (see Table 1.4). The substantial interest in polymers for various biomedical applications is mainly due to their design flexibility and the biodegradation of certain polymers at body pH. Polymers can include chemical bonds that undergo hydrolysis upon exposure to the body's aqueous environment, and they can also degrade by cellular or enzymatic pathways. The rate of biodegradation can also be controlled by manipulating the polymer properties such as hydrophobicity and crystallinity. Poly-(methyl methacrylate) (PMMA) was the first synthetic polymer used in clinical practice in 1937. Since then, numerous polymers are developed and used in a variety of orthopedic and other medical applications. They can be categorized into two types; (i) biodegradable polymers and (ii) non-biodegradable

polymers. Collagen, gelatin, poly (lactic acid) (PLA), and poly (lactic-co-glycolic acid) (PLGA) are a few notable examples of biodegradable polymers. Poly (ethylene) (PE), poly (ethylene terephthalate) (PET), and PMMA are examples of non-biodegradable polymers².

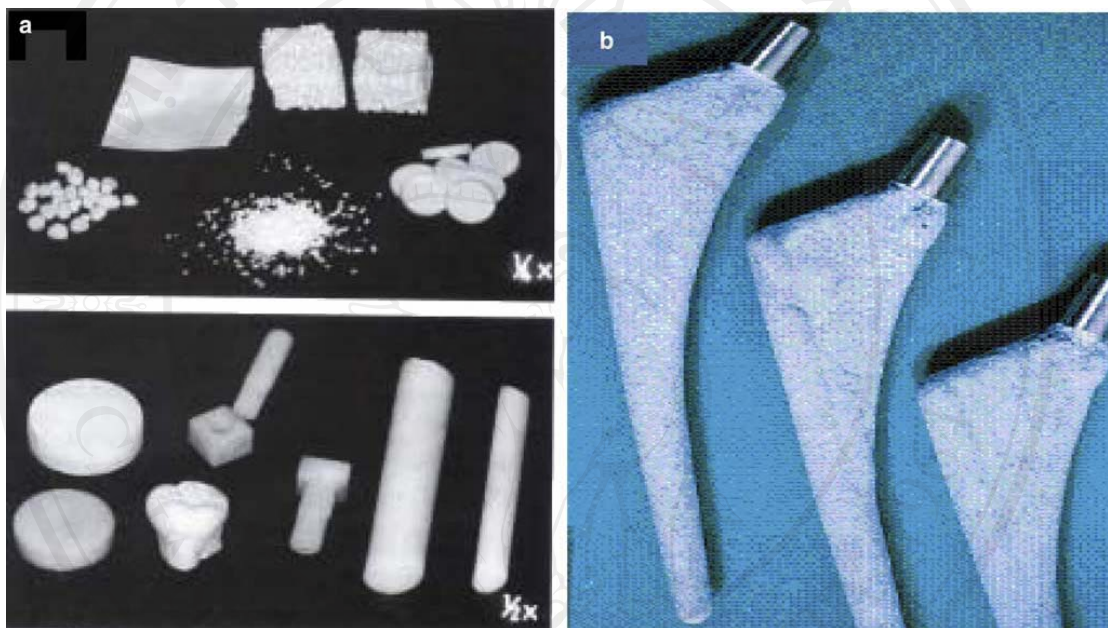


Fig. 1.6 Prototypes of HA-based bone graft materials. (a) Different shapes and sizes of HA. (b) HA-coated bioimplants².

1.5 Hydroxyapatite (HA)

The earliest attempts to replace hard tissue with biomaterials aimed to restore basic functions by repairing the defects caused by injury and disease—however the aim was to elicit minimal biological response from the physiological environment. These materials are now largely classed as “Bioinert” and the absence of a toxic response would have been considered to be a successful outcome. “Bioinert” is a term that should be used with care, since it is clear that any material introduced into the physiological environment will induce a response—however for the purposes of

biomedical implants, the term can be defined as a minimal level of response from the host tissue in which the implant becomes covered in a thin fibrous layer which is non-adherent. As with many biomedical implants, the material used in clinical application was originally designed for quite different purposes and the development of bone cement and some of the metallic alloys are prime examples of this. However, more recently, interest has been directed towards the advantageous properties of ceramics including their excellent levels of chemical resistance, compressive strength and wear resistance. In the 1920s de Jong first observed the similarities between the X-ray diffraction patterns of bone mineral and a calcium phosphate compound, hydroxyapatite. Later Posner and coworkers identified the crystallographic structure of bone mineral and hydroxyapatite. A series of studies in the 1960s, revealed that the presence of carbonate in bone and tooth mineral and hydroxyapatite may be observed directly, using infra-red spectroscopy, in the form of weak peaks between 870 and 880 cm^{-1} and a stronger doublet between 1460 and 1530 cm^{-1} and also through alterations in the hydroxyapatite lattice parameters from X-ray diffraction. The effects of the substitution of electronegative anions, such as fluorine and chlorine for (OH), were also reported to influence the lattice parameters of the structures. However, the main thrust of these studies was characterization and it was not until later in the 1960s and beyond that the development of bioactive ceramics came of age²⁹.

Hydroxyapatite ($\text{Ca}_{10}(\text{PO}_4)_6(\text{OH})_2$, HA) is a bioactive ceramics widely used as powders or in particulate forms in various bone repairs and as coatings for metallic prostheses to improve their biological properties⁹. HA is thermodynamically the most stable calcium phosphate ceramic compound at the pH, temperature and composition of the physiological fluid⁹. Recently, HA has been used for a variety of biomedical

applications, including matrices for drug release control². Due to the chemical similarity between HA and mineralized bone of human tissue, HA exhibits strong affinity to host hard tissues. Formation of chemical bond with the host tissue offers HA a greater advantage in clinical applications over most other bone substitutes, such as allografts or metallic implants^{2,3,10}.

HA possesses a hexagonal structure with a P63/m space group and cell dimensions $a=b=9.42 \text{ \AA}$, and $c=6.88 \text{ \AA}$, where P63/m refers to a space group with a six-fold symmetry axis with a three-fold helix and a microplane. It has an exact stoichiometric Ca/P ratio of 1.67 and is chemically very similar to the mineralized human bone¹². However, in spite of chemical similarities, mechanical performance of HA is very poor compared to bone. Thereby it is used only in low weight-bearing orthopedic applications, e.g., as a bone defect filler, coating-agent on metallic bioimplants, biomolecular delivery, and drug delivery. In addition, the bone mineral present a higher bioactivity compared to synthetic HA^{2-3, 10}.

Many researchers have observed that the mechanical strength and fracture toughness of HA ceramics can be improved by the use of different sintering techniques which include addition of a low melting secondary phase to achieve liquid phase sintering for better densification^{3,15-16,19}, incorporation of sintering additives to enhance densification through grain boundary strengthening^{3,10,13}. The recent trend in bioceramic research is focused on overcoming the limitations of hydroxyapatite ceramics and in improving their biological properties via exploring the unique advantages of nanotechnology. It has been established that nanotechnology offers a unique approach to overcome shortcomings of many conventional materials. From nanomedicine to nanofabrics, this promising technology has encompassed almost all

disciplines of human life. Nanostructured materials offer much improved performances than their larger particle sized counterparts due to their large surface to volume ratio and unusual chemical/electronic synergistic effects. Nanoscale ceramics can exhibit significant ductility before failure contributed by the grain-boundary phase. In 1987, Karch et al. reported that, with nanograin size, a brittle ceramic could permit a large plastic strain up to 100%. Nanostructured biomaterials promote osteoblast adhesion and proliferation, osseointegration, and the deposition of calcium containing minerals on the surface of these materials. Also, nanostructured ceramics can be sintered at a lower temperature thereby problems associated with high temperature sintering processes are also eliminated. It is possible to enhance both mechanical and biological performance of calcium phosphates by controlling characteristic features of powders such as particle size and shape, particle distribution and agglomeration. Nanoceramics clearly represent a promising class of orthopedic and dental implant formulations with improved biological and biomechanical properties³.

1.6 Nanocrystalline materials

Nanocrystalline materials, also called nanomaterials are commonly defined as those materials with very small components and/or structural features (such as particles, fibers, and/or grains) with at least one dimension in the range of 1-100 nm³³. Nanocrystalline materials are structurally characterized by a large volume fraction of grain boundaries, which may significantly alter their physical, mechanical, and chemical properties in comparison with conventional coarse-grained polycrystalline materials^{3, 30}. Fig 1.7 shows a schematic depiction of a nanocrystalline material. The

grain-boundary atoms are white and are not clearly associated with crystalline symmetry³⁰.

As the grain size is decreased, an increasing fraction of atoms can be ascribed to the grain boundaries. This is shown in Fig 1.8, where the change of the volume fraction of intercrystal regions and triple-junctions is plotted as a function of grain size. We can consider two types of atoms in the nanocrystalline structure: crystal atoms with neighbor configuration corresponding to the lattice and boundary atoms with a variety of interatomic spacing. As the nanocrystalline material contains a high density of interfaces, a substantial fraction of atoms lie in the interfaces. Assuming the grains have the shape of spheres or cubes, the volume fraction of interfaces in the nanocrystalline material may be estimated as $3D/d$ (where D is the average interface thickness and d is the average grain diameter). Thus, the volume fraction of interfaces can be as much as 50% for 5 nm grains, 30% for 10 nm grains, and about 3% for 100 nm grains³⁰.

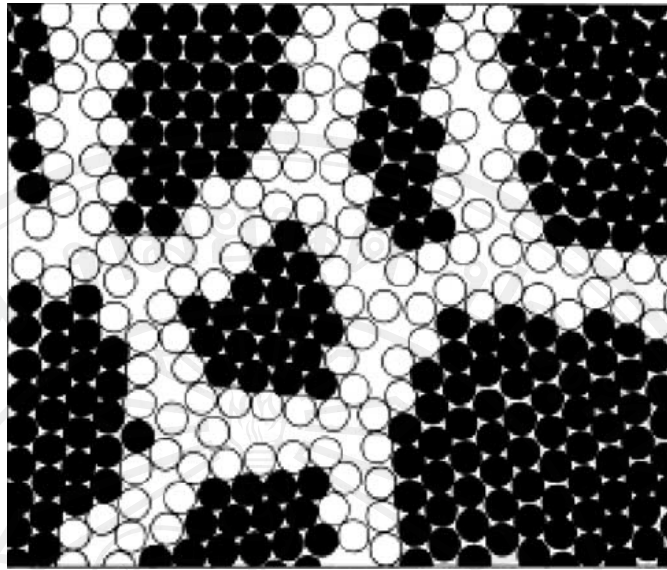


Fig. 1.7 Two-dimensional model of a nanostructured material. The atoms in the centers of the crystals are indicated in black. The ones in the boundary core regions are represented as open circles³⁰.

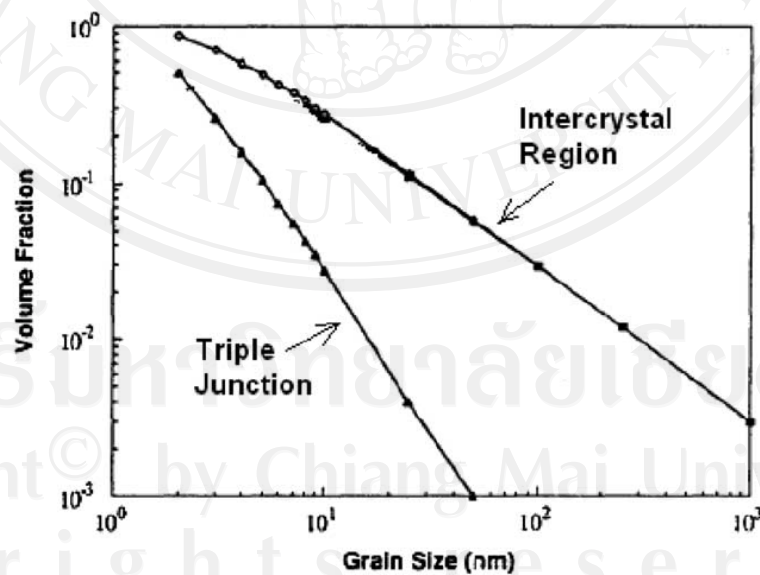


Fig. 1.8 The effect of grain size on calculated volume fractions of intercrystal regions and triple junctions, assuming a grain-boundary thickness of 1 nm^3 .

Nanocrystalline materials may exhibit increased strength/hardness, improved toughness, reduced elastic modulus and ductility, enhanced diffusivity, higher heat, enhanced thermal expansion coefficient (CTE), and superior soft magnetic properties in comparison with conventional polycrystalline materials³⁰. This has been the incentive for widespread research in this area, and lately, with the availability of advanced tools for processing and characterization, there has been an escalation of work in this field. Nanostructured materials provide us not only with an excellent opportunity to study the nature of solid interfaces and to extend our understanding of the structure–property relationship in solid materials down to the nanometer regime, but also present an attractive potential for technological applications with their novel properties. A number of techniques have surfaced over the years for producing nanostructured materials, but most of them are limited to synthesis in small quantities. There has been a constant quest to scale up the process to bulk processing, and lately, a few advances seem to hold technological promise^{30,51}.

The properties of nanocrystalline ceramics relevant to structural applications are summarized follow.

1.6.1 Reduced sintering temperature

The most obvious properties of nanocrystalline ceramics are that their sintering temperature is significantly lower than their submicron and micron-grained counterparts, once agglomeration problems are dealt with. Figure 1.9 shows up a 250 °C reduction in sintering temperature in going from a commercial $ZrO_2-3mol\%Y_2O_3$ to a nanocrystalline version⁴⁹.

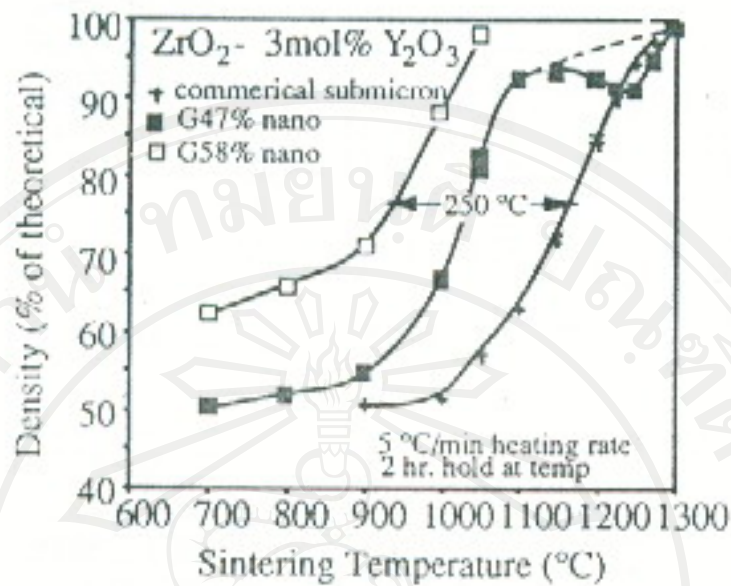


Fig. 1.9 Reduction in sintering temperature through the use of nanocrystalline grain sizes. “G” values indicate green densities⁴⁹.

1.6.2 Hardness and fracture toughness

In many cases the hardness of nanocrystalline oxide ceramics appears to be less than the reported (or measured) hardness for large-grained ceramics, however, when comparisons are made between samples with the same porosity levels, this difference almost always disappears (Fig. 1.10)⁴⁹.

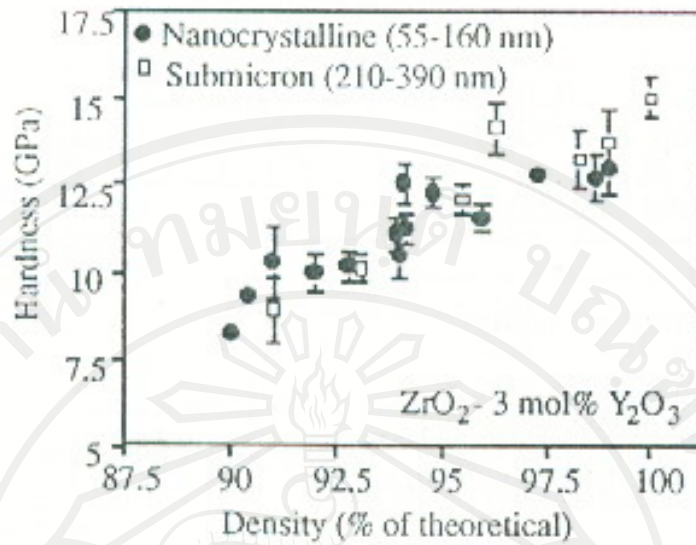


Fig. 1.10 Hardness as a function of density for nanocrystalline and submicron-grained zirconias⁴⁹.

Both TiO_2 and ZnO nanocrystalline materials were investigated with the nanoindentation technique, since only small samples could be prepared. The mechanical properties were found to vary greatly in both samples, indicating large microstructural inhomogeneity. The problem with many of the investigations of the mechanical properties of nanocompacts is that often compacts that were investigated were not dense, which makes it impossible to correlate the grain size with the mechanical properties. The density will influence the mechanical properties to a larger extent than the grain size.⁵¹

The hardness of nano-zirconia-alumina ceramics has been reported to be low compared to large-grained materials. This low value for the hardness was explained by grain boundary sliding. The low hardness values are expected to increase toughness values. This was indeed observed, when comparing nanograined zirconia-alumina with large grained composites. Toughness values of nanocrystalline ceramics

are not reported much in literature, and if so, the compacts studied were usually not dense. No systematic investigation on the influence of the grain size of dense nanoceramics on the mechanical properties has been reported⁵¹.

1.6.3 Superplasticity

Nanocrystalline materials manifest superplasticity at lower temperatures and faster strain rates than their larger-grained counterparts. The enhanced superplasticity can however disappear during deformation due to a combination of static and dynamic grain growth. Despite this limitation, applications such as near net shaping, diffusion bonding, thermally mismatched composite structures, and flaw-free processing are already under development. The high superplasticity of nanomaterials is explained by increased grain boundary sliding. Polycrystalline yttria partially stabilised zirconia (Y-PSZ) has been shown to exhibit very large elongations in high temperature deformation experiments. While tests in compression of nanophase ceramics have been carried out successfully showing extensive deformability, there is still no evidence for large elongations in tension due to the difficulties in fabricating large ceramic parts which are fully dense and maintain grain size on the nanoscale.

Recently, remarkable tensile strains were obtained in the composition 3Y-TZP+ 12 wt% Al₂O₃. A specimen could be elongated 60% after pulling at 1250°C. A maximum stress of 47 MPa was applied resulting in a maximum strain rate of $3 \times 10^{-5} \text{ s}^{-1}$.

Extensive concurrent grain growth from 30 nm up to 126 nm occurred during the test while the density decreased from 94% to 81%. It has been shown that the temperature at which superplasticity occurs was much lower for a nanocrystalline TiO₂ compact compared to larger grained compacts⁵¹.

1.7 Processing of nanocrystalline hydroxyapatite ceramics

The impact of nano HA has also been extensively reviewed with regard to recently developed manufacturing techniques. Some of the prominent processing methods for manufacturing nano HA include solid state, wet chemical, hydrothermal, mechanochemical, pH shock wave, and microwave processing (see Table 1.5), but most of them are limited to synthesis in small quantities. HA can also be processed from animal bone and coral exo-skeleton, but not on a nanoscale².

Table. 1.5 Methods involved in the synthesis of HA nanopowders²

Methods	Grain size (nm)	General remarks
Solid state	500	Inhomogeneous, large grain size (micro to nano), irregular shapes, reaction condition 900–1300 °C
Wet chemical	20–200	Nanograin size, low crystallinity, homogeneous, reaction condition: room temperature to 100 °C
Precipitation/hydrothermal	10–25	Homogeneous, ultra-fine particles, low crystallinity, reaction condition: room temperature to 200 °C (1–2 MPa)
Hydrothermal	10–80	Homogeneous, fine crystals, high temperature, and high-pressure atmosphere
Mechanochemical	<20	Easy production, semi-crystallinity, ultra-fine crystals, room temperature process
pH shock wave	20–100	High-energy dispersing, nonporous, monocrystalline particles with Ca/P molar ratio 1.43–1.66
Microwave	100–300	Uniformity, nanosize particles, time and energy saving

All of these methods produce HA powder cannot be controlled the agglomeration during synthesis or drying or at the processing step. Agglomeration can make the lower sintered density as well as crack-like voids during densification. Thus, to produce sintered HA with good mechanical properties, one need to use agglomerate-free fine HA powder with high surface area.

1.7.1 Densification characteristics of nanocrystalline powders

A major problem in the processing of nanophase oxide powders is the existence of agglomerates in these powders and as a result the formation of relatively large interagglomerate pores during pressing (Fig. 1.11)^{45,49}.

While small interparticle pores are easily closed during sintering, large interagglomerate pores need high sintering temperature or long sintering times to be eliminated. Pores exceeding a critical sized will even grow during sintering. Hence significant grain growth will take place^{45,49}.

One possible way to overcome this problem is the use of novel sinter techniques, such as hot-pressing, hot isostatic pressing, spark plasma sintering, sinter forging, non-isothermal sintering, ultra-rapid sintering, microwave sintering, and selective sintering etc. Conventional pressureless sintering is the most common low cost approach to sinter ceramics in those methods. Unfortunately, in the pressureless sintering, both processes of the densification and grain growth are driven by diffusion.

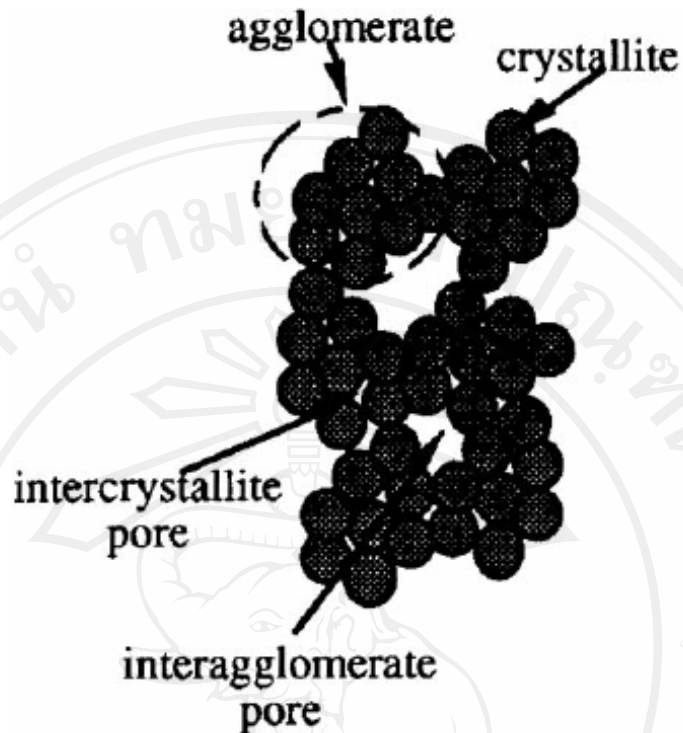


Fig. 1.11 Schematic diagram of an agglomerated powder^{45,49}.

1.7.1.1 Minimizing grain growth and maximizing densification during sintering of ultrafine particles.

The temperature of the green compact has to be raised until significant diffusion starts to take place. Unfortunately, the fact that diffusion is required for densification leads to a fundamental problem, since grain growth occurs by the same mechanism. Therefore sintering strategies have to be used that promote densification but do not stimulate grain growth as well. The densification and grain growth processes have to be decoupled^{45,49,51}.

1.7.1.2 The sintering of nanopowders (nanosintering)

Thermodynamically, powders are unstable due to the large surface area. Nanoparticles adopt different surface energies compared to larger particles, for instance, by a different local atomic arrangement at the surface. Kinetically, sintering of nanopowders is significantly enhanced. Sintering of many nanocrystalline powders indicated depressed sintering onset temperatures ($0.2-0.3T_m$) as compared to microcrystalline powders ($0.5-0.8T_m$). Pressureless sintering is an easy, the most common and cheapest sintering method to be used. Conceptually, sintering three stages, as is shown in Fig. 1.12, in the first stage, necks are formed by diffusion between adjacent, touching particles. The neck formation increases the mechanical strength of the compact, but does not lead too much densification³¹. Molecular dynamics simulations indicated extremely fast sintering behaviour for nanoparticles, that can not be explained by surface diffusion only. Other mechanisms have been proposed to account for this fast sintering behaviour. It has been speculated that in this first stage a major difference arises between nano and larger grained materials, in that fast surface diffusion may allow the small grains to slip past one another along the grain boundaries and rearrange in a more packing efficient manner. TEM studies of nanoparticles confirmed that after neck formation the adjacent particles rotate to achieve a minimum in grain boundary energy. At this point, the contribution of various diffusion mechanisms or a change in the sintering mechanism is possible, at least in the initial densification stage⁵¹.

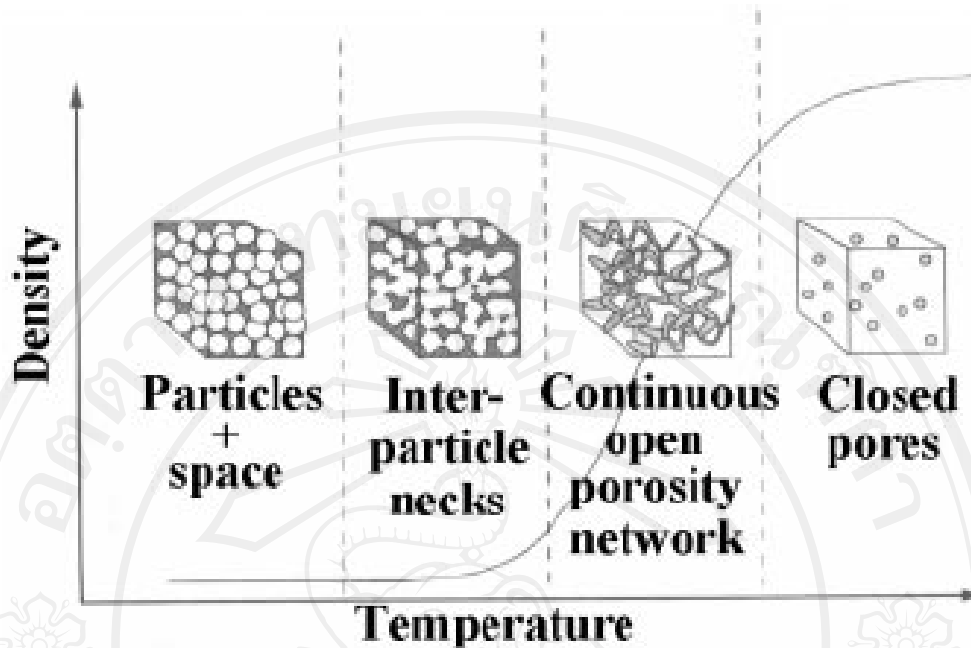


Fig. 1.12 Different stages in densification of compacts⁵¹.

After the first sintering stage the ceramics contain an interpenetrating network of tubular open pores. In the second stage the density increase to approximately 90%. In the ideal case, the open tubular pores shrink in radius but not in length, thereby leading to sample densification until the pores have such a small diameter/length ratio that they ultimately collapse due to Raleigh instabilities. By virtue of localised collapse, the open tubular pores then form closed spherical pores. The gradual shrinkage and elimination of these closed pores then marks the third and final stage of sintering. This general process is the same for ceramics with nanosized and larger grains. The most common problem in sintering of nanoparticles (nanosintering) is the elimination of large pores that originate from the green compact. The conventional thermodynamic treatment of the pore shrinkage was applied to nanoceramics sintering by Mayo in 1996³¹. The critical pore-to-grain size ratio concept that applies to

sintering of coarsegrained compacts also is applicable for sintering of nanocompacts. That is pores smaller than the critical size will shrink, while larger pores undergo pore-boundary separation. Mayo developed a modified sintering law that directly accounts for pore size effects on densification rate⁵¹:

$$\frac{1}{\rho(1-\rho)} \frac{d\rho}{dt} \propto \frac{1}{d^n} \frac{1}{r} e^{\left(-\frac{Q}{RT}\right)} \quad (1)$$

When, ρ = density, d = particle size, n = constant depending on the sintering mechanism, r = pore radius, Q = activation energy, R = gas constant, T = absolute sintering temperature.

This equation predicts that the highest densification rate occurs for the finest pore size. A small pore size is also critical in controlling the final grain size based on the pore pinning effect. For these purposes, a small and uniform pore population is desired in the green compact. It has also been shown that open pores severely inhibit grain growth. When the density becomes higher than 90%, grain sizes increase rapidly during sintering. Grain growth follows a conventional rate law⁵¹:

$$G^n - G_0^n = kt \quad (2)$$

When, G = instantaneous grain size, G^0 = initial grain size, k = rate constant with an Arrhenius dependence, t = time, n = grain-growth exponent. The value of n has been reported to vary from 1 to 20 for different nanomaterials, but also varied for the same compact in the different densification regimes, which makes the predictable value of this equation rather low⁵¹.

Skorokhod and Ragulya (1998) were reported the novel nonisothermal sintering techniques with rate-controlled sintering for consolidation of nano-size powders⁴⁹.

Kim et al. prepared nanocrystalline indium tin oxide powder with different particle size using a coprecipitation process. They examined the sintering characteristics of the powder at different heating rates. Decrease of particle size in nanosized powder regime promoted the densification in normal rate sintering as temperature increased, while this was shown to retard severely the densification at high temperature in rapid rate sintering³⁰.

Yoshimura et al 1999 reported that a high heating rate exhibited more enhanced densification than slow sintering and also lead to smaller grain size at full density. It is not clear why in this case the high heating rate was beneficial. It may be that the microstructure was more homogeneous, allowing higher heating rates³⁰.

Kim et al. employed two-step sintering method to consolidate nanosize BaTiO₃ powders. This comprised initial heating at relatively higher temperature and following low-temperature sintering for a long period of heating. Pressed green bodies of BaTiO₃ were first heated to 1300°C to achieve an intermediate density, then cooled down and held at 1100°C for 0–20 h until they became fairly dense. Slight grain growth was shown to occur during the second step (with the final grain size of 1 μm), whereas the density was shown to decrease significantly³⁰.

Ragulya reported synthesis of nanocrystalline powders of barium barium titanate by non-isothermal and rate-controlled decomposition of organic precursors. The nanograined barium titanate powder sintered under rate-controlled conditions produced dense and fine-grained ceramic and it was pointed out that the thermal activated processes should be optimal through the entire temperature–time processing schedule³⁰.

Duran *et al.* prepared powders of yttria-doped tetragonal zirconia (3 mol %) with a narrow pore size distribution and ultrafine particle size (~9 nm) by the mixed organic and inorganic precursors coprecipitation method. The compaction behavior of almost agglomerate-free calcined powders was studied, and their sintering behavior using both isothermal and non-isothermal techniques were evaluated³⁰.

Han *et al.* (2004)²⁶ was synthesized nanocrystalline HA powder by citric acid sol-gel combustion method. After sintering in air at 1200°C the grain size is about 3 μm, and the flexural strength is 37 MPa.

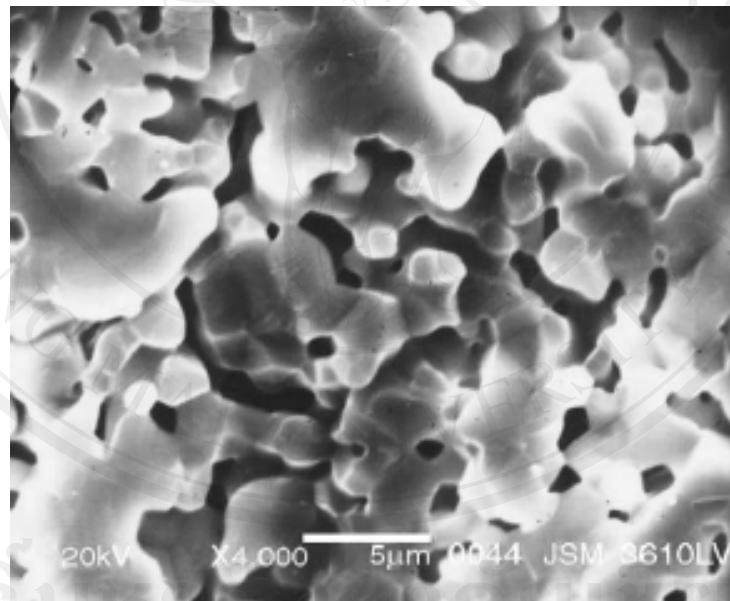


Fig. 1.13 SEM micrograph of the resulting bioceramic sintered 1200°C for 3 h²⁶.

Shu *et al.* (2005)²⁴ have been synthesized nanocrystalline HA powder by gelatin-based precipitation method and then uniaxially pressed at 10 MPa followed by cold isostatic pressing at 180 MPa. The green compacts were sintered at a temperature of 1200 °C for 4 h in air in a furnace. The SEM picture of fracture surface is shown in

Fig. 2.13. There are many micropores with irregular shape. The formation of pores is beneficial, as they would permit the circulation of the physiological fluid throughout them.

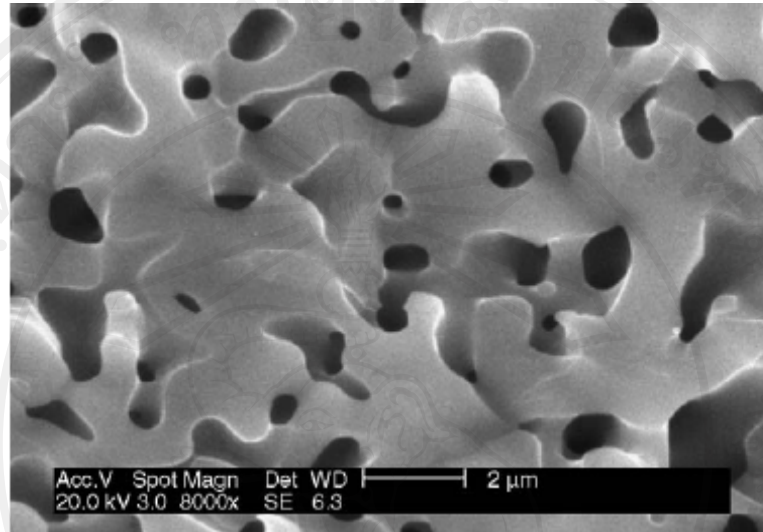


Fig. 1.14 SEM micrograph of the fracture surface for samples sintered at 1200°C²⁴.

Ashis *et al.* (2006)²⁸ was studies effect of nanopowder morphology, which HA synthesized from reverse micelle template system, on densification at 1250°C with different amount of rod-shaped and spherical nanopowders ratios. It was observed that an increase in high aspect ratio powder content in the compacts decreased sintered density under pressureless sintering condition. Also, due to excessive grain growth, no nanoscale morphology could be retained in the sintered microstructure.

It have review been that the HA derived either from natural source or from synthetic source is regarded as bioactive substance, and hence it is recognized as a good bone graft material. Thus, the HA produced from natural bovine bone with calcinations method could be an inexpensive alternative and many researcher had have synthesized hydroxyapatite from bovine bone, but on microscale^{9,17,25}.

Focusing on HA ceramic systems, there are three main challenges to achieving the goal of fabricating engineering components from HA nanopowders, namely:

- The low-cost production of quantities of nanopowders with controlled agglomeration⁵²;
- The compaction of the particles to achieve flaw-free, homogeneous, high green density bodies prior to sintering (i.e. avoiding cracks, pores and density gradients)⁵²; and
- The maximisation of densification and minimisation of grain growth during sintering⁵².